Structure and function of the voltage sensor of sodium channels probed by a beta-scorpion toxin.

Sandrine Cestèle, Vladimir Yarov-Yarovoy, Yusheng Qu, François Sampieri, Todd Scheuer, William A. Catterall

STRUCTURE AND FUNCTION OF THE VOLTAGE SENSOR OF SODIUM CHANNELS PROBED BY A β-SCORPION TOXIN

Sandrine Cestèle[1], Vladimir Yarov-Yarovoy[1], Yusheng Qu[1], François Sampieri[2], Todd Scheuer[1] and William A. Catterall[1]

[1]Department of Pharmacology, University of Washington, Seattle, WA 98195-7280, USA, and [2]Université de la Méditerranée, I.F.R. Jean Roche, CNRS FRE 2738, Bd Pierre Dramard, 13916 Marseille, France

Address correspondence to: William A. Catterall, Department of Pharmacology, University of Washington, Seattle, WA 98195-7280, Tel. 206 543-1925; Fax. 206 543-3882; E-mail: wcatt@u.washington.edu

Voltage sensing by voltage-gated sodium channels determines the electrical excitability of cells, but the molecular mechanism is unknown. ß-scorpion toxins bind specifically to neurotoxin receptor site 4 and induce a negative shift in the voltage dependence of activation through a voltage-sensor trapping mechanism. Kinetic analysis showed that β-scorpion toxin binds to the resting state and subsequently traps the voltage sensor in the activated state in a voltage-dependent, but concentration-independent manner. Mutations of E779 in extracellular loop IIS1-S2 and both E837 and L840 in extracellular loop IIS3-S4 reduce the binding affinity of ß-scorpion toxin. Mutations of positively charged and hydrophobic amino acid residues in the IIS4 segment do not affect β-scorpion toxin binding, but these mutations alter the voltage dependence of activation and enhance ß-scorpion toxin action. Molecular modeling with the Rosetta program and docking of β-scorpion toxin yielded a three-dimensional model of the toxin-receptor complex with the IIS4 voltage sensor, which is formed at the extracellular surface of the protein. Our results define the position of the voltage sensor in the resting state of the sodium channel and favor voltage-sensing models in which the S4 segment spans the membrane in both resting and activated states.

The voltage-gated ion channels and their structural relatives are a large superfamily of membrane proteins specialized for electrical signaling and ionic homeostasis (1). Voltage-gated sodium channels are responsible for the increase in sodium permeability that initiates action potentials in electrically excitable cells (2) and are the molecular target for several groups of neurotoxins, which bind to different receptor sites and alter voltage-dependent activation, conductance, and inactivation (3,4). Sodium channels are composed of one pore-forming α subunit of about 2000 amino acid residues associated with one or two smaller auxiliary subunits, β1 – β4 (5-7). The α subunit consists of four homologous domains (I-IV), each containing 6 transmembrane segments (S1-S6), and a reentrant pore loop (P) between S5 and S6 (5). The S4 transmembrane segments are positively charged and serve as voltage sensors to initiate channel activation (8-14). However, the molecular mechanism of voltage sensing by sodium channels and the other members of the voltage-gated ion channel family is unknown.

The initial 'sliding helix' (9) or 'helical screw' (15) models for voltage sensing proposed that the S4 segments, which have positively charged amino acids at intervals of three residues, transport gating charges outward to activate sodium channels in response to depolarization by moving along a spiral pathway through the protein structure. This movement would preserve interactions with surrounding hydrophilic and negatively charged amino acid residues during gating and thereby stabilize the gating charges in the intramembrane environment. Much experimental support has been developed for this general model. Mutation of the S4 arginines reduces the steepness of voltage-dependent gating of Na^+ and K^+ channels, consistent with their role as gating charges (10,16-18). Ion pairing of arginines with negatively charged amino acid residues in the S2 and S3 segments is required for biosynthesis and cell surface expression of a K^+ channel (17). Outward movement and rotation of

the S4 segments has been detected by chemical modification and fluorescent labeling of Na^+ and K^+ channels (11,19,20). The extents of chemical modification of gating charges in resting and activated states imply that only a narrow waist of the S4 segment is covered by the channel protein (21,22), and the requirement for placement of functional gating charges at each third position in the S4 voltage sensor rather than at other positions also is best explained by movement of the S4 segments through a pathway in which specific, sequential protein-protein interactions are made (23). Substitution of histidine residues for the arginine gating charges in S4 segments of a K^+ channel created a voltage-dependent proton permeation pathway (24). Moreover, mutation of gating charges in the S4 voltage sensors of Na^+ or K^+ channels is sufficient to allow cation permeation through a gating pore (25,26), demonstrating that cations can permeate through a modified gating pore. A low-resolution structure of a sodium channel suggests peripheral pores in each domain that may serve to move voltage sensors through the protein across the membrane (27).

In contrast to these accumulated structure-function data, x-ray crystallographic studies of a bacterial voltage-gated K^+ channel in complex with detergent and a site-directed antibody revealed a structure in which the S3 and S4 segments lay along the position of the intracellular surface of the membrane, dissociated from the remainder of the protein (28-30). These results led to the concept that the voltage sensors function as loosely linked 'paddles', pivoting through the phospholipid surrounding the core of the ion channel as a semi-rigid body rather than moving gating charge outward through the protein structure. This 'paddle' model makes strikingly different predictions for polypeptide toxins that modify gating by interaction with the voltage sensors. Whereas polypeptide toxins might be able to bind the extracellular end of the voltage sensors in the resting state in a 'sliding helix' or 'helical screw' gating model, the S4 segments would not be expected to be available for toxin binding in the resting state in the 'paddle' model.

Scorpion venoms contain two groups of polypeptides toxins that alter sodium channel gating. The α-scorpion toxins, as well as sea anemone toxins and some spider toxins, bind to neurotoxin receptor site 3 and slow or block sodium channel inactivation (31-34). Amino acid residues that contribute to neurotoxin receptor site 3 are localized in the S3-S4 linker in domain IV (35) and in the large extracellular loops in domains I and IV (36,37). Binding of toxins to IVS3-S4 is thought to slow inactivation by preventing the normal outward movement of the IVS4 transmembrane segment during channel gating (35,38). Polypeptide toxins that inhibit activation of K^+ channels and Ca^{2+} channels bind to a similar motif in their S3-S4 loops and are thought to act in a similar manner (39,40) (and see Discussion).

In contrast to these toxins that inhibit activation or inactivation gating, ß-scorpion toxins bind to neurotoxin receptor site 4 on sodium channels and enhance activation by shifting its voltage dependence to more negative potentials (41-48). Our previous results (48) implicate the extracellular loops S1-S2 and S3-S4 in domain II in formation of neurotoxin receptor site 4. Moreover, a voltage sensor-trapping mechanism, in which the bound β-scorpion toxin holds the IIS4 segment in its outward, activated position was proposed to account for enhancement of activation (48,49). Thus, these toxins provide unique molecular probes of voltage-sensing mechanisms of sodium channels. Here we show that a β-scorpion toxin binds to its receptor site in the resting state and traps the voltage sensor in its activated state via a voltage-dependent but concentration-independent mechanism. We identify individual amino acid residues in the toxin-receptor interaction site, develop a three-dimensional structural model of toxin binding, and map the effects of mutations in the IIS4 voltage sensor on gating and toxin action. Our results strongly favor voltage-sensing models in which the S4 segment is in a transmembrane position in both the resting and activated states of the channel and thus argue against the paddle model of gating.

Materials and Methods

Materials - ß-scorpion toxin Css IV was purified form the venon of *Centruorides suffusus suffusus* (50). The pCDM8 vector and the MC1061 *E. coli*

bacterial strain were purchased from Invitrogen. Human embryonic kidney tsA-201 cells, a simian virus (SV-40) large T-antigen expressing derivative of HEK-293 cells, were provided by Dr. Robert Dubridge (Cell Genesis, Foster City, CA). cDNA encoding rat $Na_v1.2a$ α subunits (51,52) in the pCDM8 vector was used for sodium channel expression.

Site directed mutagenesis - Mutations E779Q, I830A, V831A, S832-834-847-851A, E837Q, R850Q, R853Q, K859Q and K862Q were produced using an M13 construct containing a XmaI-SphI fragment (nt 541-1,897) of the $Na_v1.2a$ cDNA. Uracil-containing mutagenesis template was prepared from this construct and oligonucleotide-directed mutagenesis was performed using the dut^- ung^- selection procedure (53). Mutations made in the M13 construct were confirmed by sequencing, excised by restriction at the sites XmaI-SphI and isolated by low melting point agarose gel electrophoresis and Prep-a-gene (BioRad Inc.). Fragments were then subcloned into the Nav1.2 sodium channel cDNA in pCDM8. The mutations were confirmed in the final constructs by DNA sequencing using the ABI Prism dye terminator cycle sequencing kit (Perkin-Elmer Applied Biosystems). All of the other mutants were amplified by PCR in an 800-bp cDNA fragment extending from the XmaI site to the SphI site and were subcloned into the $Na_v1.2a$ cDNA in pCDM8. To facilitate the screening of the clones, a silent restriction site was introduced along with the mutation: MseI for M778C, E779C, M783C; HpaI for E837C, L838C, L840C; N842A, L846C, V848A, L849C, F852C, L854C, L855C, V857C, F858C and L860C. All clones were sequenced through the entire PCR fragment.

Measurements of β-scorpion toxin binding in transfected tsA-201 cells - The tsA-201 cells were maintained at 37^{O}C in 10% CO_2 in DMEM/Ham's F12 medium (GIBCO BRL and Life Technologies) supplemented with 10% fetal bovine serum, 20 µg/ml penicillin, and 10 µg/ml streptomycin FBS (Gemini Biological Products). For transient expression of sodium channels for ^{125}I-Css IV binding, tsA-201 cells were subcultured in 150-mm tissue culture plates one or two days before transfection. Cells were transfected with 50 µg of pCDM8 vector containing the Nav1.2a sodium channel cDNA by using calcium phosphate/DNA co-precipitation (54). Cells were collected for membrane preparation 40-48 h after transfection. Membranes were prepared and specific binding of ^{125}I-Css IV toxin was measured as previously described (48).

Electrophysiological recording and analysis - Transient expression for electrophysiological analysis of sodium channels was done by calcium phosphate-mediated co-transfection of tsA201-cells in a 35-mm dish with a 10:1 molar ratio of sodium channel plasmid and pEBO-pCD8-leu2, a vector encoding the CD8 antigen as described (54). Transfected cells were subcultured on the day following transfection, then analyzed 40-72 h after transfection. Cells expressing the CD8 antigen were identified by incubation with polystyrene microspheres precoated with anti-CD8 antibody and used for electrophysiological recordings.

Whole-cell sodium currents were recorded from tsA-201 cells expressing Nav1.2a wild-type or mutant α subunits. Recording solutions (in mM): Extracellular: 150 NaCl, 10 Cs-HEPES, 1 $MgCl_2$, 2KCl and 1.5 $CaCl_2$, pH 7.4. Intracellular: 190 N-methyl-D-glutamine, 10 HEPES, 4 $MgCl_2$, 10 NaCl and 5 EGTA, pH 7.4. For the experiments of Figs. 1 and 2, the following solutions were used: Extracellular: 140 NaCl, 5 CsCl, 1.8 $CaCl_2$, 1 $MgCl_2$, 10 HEPES, pH 7.4; Intracellular: 90 CsF, 50 CsCl, 10 CsEGTA, 10 NaF, 2 $MgCl_2$, 10 HEPES, pH 7.4. Patch electrodes were pulled from 75 µl micropipette glass (VWR Scientific) and were fire-polished before use. Electrode resistances were typically 1.5-2.5 mΩ in the bath. Recordings were obtained using an Axopatch 1C Amplifier (Axon Instruments). Voltage pulses were applied and data were acquired using Pulse software (Heka, Lambrecht, Germany). Linear leak and capacitance currents have been subtracted using an online P/-4 subtraction paradigm. Css IV was dissolved in the extracellular solution at the final concentration and placed in the recording bath. All experiments were performed at room temperature. Conductance voltage-curves were derived from peak sodium current versus voltage

measurements according to : $G=I/(V-V_R)$ where I is the peak current, V is the test voltage and V_R is the apparent reversal potential. Normalized conductance-voltage curves were fit with a Boltzmann relationship of the form $1/(1/\exp((V_{1/2}-V)/k))$ or with the sum of two such expressions, where V_a is the voltage for half-maximal activation and k is a slope factor expressed in mV.

Sequence alignment, homology and de novo structural modeling - Rat $Na_v1.2$ channel domain II segments S1 through S4 sequence (residues L754-G875) was aligned with KvAP channel (55) segments S1 through S4 sequence (residues D33-D159) using ClustalX software (56). The alignment of segments S3 and S4 was then manually adjusted using the KvAP channel voltage-sensor structure ((29), pdb code:1ORS) to fit experimental observations showing that residues E779, E837, and L840 of the Na^+ channel form the receptor site for the β-scorpion toxin and that positively charged residues on the sodium channel S4 segment are not important for binding of the toxin (see Results). β-scorpion toxin sequence was aligned with neurotoxin 2 sequence ((57), pdb code: 1JZA) using Clustal X software (56). Residues in the sequence alignments shows in Results were colored with Jalview (58) using the Zappo color scheme, where hydrophobic residues (I, L, V, A, and M) are colored pink, aromatic residues (F, W, and Y) are colored orange, positively charged residues (K, R, and H) are colored blue, negatively charged residues (D and E) are colored red, hydrophilic residues (S, T, N, and Q) are colored green, P and G colored magenta, and C is colored yellow. Homology and de novo modeling was performed using the Rosetta program (59-62). Briefly, 1000 models were generated followed by model clustering. The best model was chosen as a center of the biggest cluster, defined as having the lowest standard mean deviation value (between positions of C-alpha atoms of all residues) to all other models in a cluster. After failed attempts to generate a docking model that would fit most of the experimental data using original KvAP structure backbone coordinates, the best Na^+ channel homology/de novo model was manually adjusted to create larger space for CssIV to bind in the extracellular lumen between transmembrane segments S1-S2 and S3-S4 by adjusting the ψ torsion angle by -10^o at position G822 (Fig. 8), so that Cα of V843 in the S3-S4 loop moved away from the S1-S2 loop by ~5 Å. Docking simulations of the β-scorpion toxin binding to the $Na_v1.2$ channel domain II S1-S4 segments were performed using Rosetta-Dock program (63). Five thousand models were generated followed by model clustering, and the best model was chosen as the lowest scoring model among the top 3 clusters.

RESULTS

Binding of Css IV toxin to the resting state - Incubation of tsA-201 cells expressing sodium channels with Css IV toxin at a negative membrane potential has no effect on sodium channel function, but strong depolarization to fully activate sodium channels in the presence of Css IV toxin strongly enhances the activation process by shifting its voltage dependence negatively by 32 mV (48). We hypothesized that this process involves a two-step toxin action: binding to sodium channels without functional effect on activation at the resting membrane potential followed by trapping the IIS4 voltage sensor in its activated conformation upon channel activation in the presence of bound toxin (48). The voltage-sensor trapping model of β-scorpion toxin action (48) implies that the toxin initially binds to the resting state of the channel and subsequently binds the activated IIS4 voltage sensor with high affinity to trap it in its activated state. In our previous experiments, we measured concentration-dependent toxin binding directly using radioligand-binding methods, but sequential binding to the resting state and subsequent voltage-sensor trapping was not directly demonstrated. To address this key point, we allowed Css IV toxin to bind to sodium channels in transfected cells under whole-cell voltage clamp, and we measured the rapid kinetics of its voltage-sensor trapping action by strongly depolarizing for a brief period and then determining the sodium currents elicited by a test pulse to a negative membrane potential at which only toxin-modified channels can activate. If rapid voltage-sensor trapping follows slow binding to

the resting state, the negatively shifted activation of the channel should develop rapidly upon depolarization and be concentration-independent in this experimental protocol. After binding of Css IV toxin, a strong, brief prepulse to +50 mV for 1 ms caused a large increase in sodium currents in subsequent test pulses to -50 mV or -45 mV (Fig. 1a, b), and these toxin-modified sodium channels activated much more rapidly than unmodified sodium channels (Fig. 1a, b, scaled dotted lines). In contrast, these sodium channels activate at -40 mV and -35 mV without a prepulse but activation is still accelerated significantly after the prepulse in the presence of toxin (Fig. 1c, d). No such acceleration of activation by depolarizing prepulses is observed in the absence of toxin (data not shown). These results indicate that sodium channels are modified by bound Css IV during 1-ms depolarizing pulses, and the modified channels immediately respond to a test depolarization with rapid activation of sodium current. Evidently, toxin binding has occurred before the prepulse, and then pre-bound toxin can trap the voltage sensor during the depolarization within 1 ms.

If toxin binding does indeed occur before voltage-sensor trapping, the effect of the toxin during the depolarizing prepulse should be concentration-independent. To test this prediction, the time course of development of the toxin-modified population of channels was measured in the presence of either 40 nM or 400 nM Css IV toxin. Cells were depolarized to a prepulse potential of +20 mV for a variable time from 0.1 to 1.4 ms, and the activation of sodium currents was measured in a subsequent test pulse to -65 mV where only toxin-modified channels are activated (Fig. 2a, b). Fitting the resulting data to a single exponential equation yielded time constants for toxin action of 0.48 ms at 40 nM and 0.53 ms at 400 nM (Fig. 2c), demonstrating that toxin action during the depolarizing prepulse is concentration-independent. Similar results were obtained for prepulses to 20 mV, 50 mV, and 80 mV (Fig 2d). Evidently, β-scorpion toxins bind to sodium channels in the resting state in a concentration-dependent manner, as observed in our previous ligand binding studies (48), and the pre-bound toxin traps the voltage sensor in its activated conformation in a rapid, concentration-independent, zero-order interaction after activation of the channel.

Amino acid residues in the β-scorpion toxin receptor site - Studies of β-scorpion toxins identified positively charged and hydrophobic amino acids as important residues for toxin binding (64-66), suggesting interactions with hydrophobic and negatively charged amino acid residues in the sodium channel. Our previous experiments with sodium channel chimeras implicated the extracellular loops S1-S2 and S3-S4 as well as transmembrane segment S4 of domain II in the formation and function of the β-scorpion toxin receptor site on voltage-gated sodium channels (48,49). To identify individual amino acid residues required for high-affinity β-scorpion toxin binding, we introduced single point mutations in the IIS1-S2, IIS3-S4 and IIS4 segments of $Na_v1.2a$ channels by site-directed mutagenesis (Fig. 3). The binding affinity of each of the mutants for the β-scorpion toxin Css IV was tested in competitive toxin displacement experiments using membranes prepared from tsA-201 cells expressing the mutant sodium channel α subunits (Fig. 3a, b). All mutations except L846C had a level of functional expression that was sufficient for analysis in binding experiments. Mutations of three amino acid residues caused a reduction of binding affinity for Css IV from 3.5- to 5.6-fold--E779Q/C in IIS1-S2 (Fig. 3a, c) and E837Q/C/R and L840C in IIS3-S4 (Fig. 3b, c). The K_d values determined from Scatchard analysis of the binding data for all of the mutants are illustrated as a bar graph in Fig. 3c. None of the mutations of hydrophobic residues in the IIS4 segment changed the affinity of the toxin for its receptor site significantly (Fig. 3c), similar to the lack of effect observed previously for mutations of the positively charged residues in this helix (49). Evidently, E779, E837 and L840 in extracellular loops IIS1-S2 and IIS3-S4 are involved in the formation of the β-scorpion toxin receptor site, but the S4 segment is not. These results suggest that Css IV binds to these two extracellular loops in domain II through a combination of electrostatic and hydrophobic interactions with the negatively charged and hydrophobic side chains of these amino acid residues.

Functional Effects of Css IV toxin on mutants E779Q, E837Q and L840C - To determine the functional properties of E779Q, E837Q and L840C mutants, wild-type, and mutant $Na_v1.2$ channels were transiently expressed in tsA-201 cells and analyzed by whole-cell voltage clamp. In the absence of toxin, analysis of the conductance-voltage relationships for the wild-type and mutant channels showed a positive shift in the activation curve for E779Q, E837Q and L840C of 6 to 17 mV (Fig. 4a, Supplementary Table 1). The three mutations also reduced the steepness of the activation curve. Therefore, despite the location of these mutations in the extracellular loops S1-S2 and S3-S4 in domain II, voltage-dependent activation initiated by the S4 segments is altered.

As previously described for wild-type $Na_v1.2$ channels (48,49), treatment with 200 nM Css IV induced a negative shift in the voltage-dependence of activation of a fraction of $Na_v1.2$ channels following a brief depolarizing prepulse to 50 mV (Fig. 4a and (48,49)). This effect is revealed in these experiments as a negatively shifted foot of the activation curve (Fig. 4a, open vs. closed circles), and the fraction of sodium channels with shifted activation is quantified by fit to a two-component Boltzmann equation. In the presence of 200 nM Css IV, the voltage-dependence of activation of E779Q and L840C was not altered following a prepulse, indicating complete block of toxin binding and action at this concentration (Fig. 4b, d, open symbols). Higher concentrations of toxin can cause a negative shift of sodium channel activation, indicating that Css IV can alter gating of these channels if sufficient toxin is present to bind to their receptor site (e.g. Fig. 4d, gray diamonds, for 1 μM Css IV). On the other hand, E837Q channels activate at more negative potentials in the presence of 200 nM Css IV toxin (Fig. 4c). However, the fraction of toxin-modified E837Q channels was reduced compared to wild-type; 200 nM Css IV modifies only 8% of E837Q channels versus 14% of wild-type channels (Fig. 4a, c). These results indicate that E779Q, E837Q, and L840C mutations reduce the affinity of the toxin Css IV for its receptor site, which also reduces the effect of the toxin on sodium channels. Thus, these three amino acid residues appear to interact directly with the β-scorpion toxin and are critically involved in its functional effects.

Role of the hydrophobic residues of the IIS4 segment in sodium channel activation - Our previous studies suggested that β-scorpion toxins act on sodium channel activation through a voltage-sensor trapping mechanism (48,49). Neutralization of the two outermost positive charges of the IIS4 segment enhances the effect of the toxin on sodium channel activation (49). To further examine the role of the IIS4 segment on β-toxin action, we analyzed the activity of Css IV on mutants in which each of the hydrophobic residues of the IIS4 segment were mutated to cysteine or alanine. In the absence of toxin, analysis of the conductance-voltage relationships indicates that seven of these eight mutations shift the voltage-dependence of sodium channel activation to more positive potentials (Fig. 5, Supplementary Table 1). The strongest effect on the voltage dependence of activation is observed with the mutant L860C, which shifted the activation curve +18.4 mV (Fig. 5d), similar to the effect of the mutation L860F that was studied previously (51). In contrast, the mutant L854C activates at 5.6 mV more negative membrane potentials (Fig. 5c, Supplementary Table 1). The steepness of the activation curve is reduced for all the IIS4 mutants (Fig. 5, Supplementary Table 1). These results indicate an important role for all of these hydrophobic amino acid residues in the voltage-sensing function of the IIS4 segment.

As for the wild-type $Na_v1.2a$ channels, 200 nM Css IV induced activation of the sodium channels with mutations in the IIS4 segment at more negative membrane potentials (Fig. 6, Supplementary Table 2). However, for the mutants V848A, F852C, L854C and V857C, a larger shift of the activation curves is induced by 200 nM Css IV than for wild-type (Fig. 6, Supplementary Table 2). Css IV (200 nM) modified the voltage dependence of 21 to 27% of these mutant channels versus 14% for the wild type channels. More remarkably, for the mutant L854C, Css IV caused a shift of the activation of 22% of $Na_V1.2$ channels without a depolarizing prepulse, and a shift of the activation of 27% of $Na_V1.2$ channels was observed after a prepulse (Figs. 6c). The effects of

mutations in the positively charged amino acid residues (49) and in the hydrophobic amino acid residues (Figs. 5, 6) in transmembrane segment IIS4 on the ability of β-scorpion toxin to shift the voltage dependence of activation before and after a positive prepulse are illustrated as bar graphs in Fig. 7. The charged S4 residues are arranged in a diagonal stripe on the surface of the IIS4 α helix when viewed as a helical net (Fig. 7a). Most substitutions of residues in IIS4 shift the voltage dependence of activation toward more positive potentials, indicating that the normal amino acids at these positions stabilize the activated state of the channel (Fig. 7b). Most of these mutations of hydrophobic residues in IIS4 also increase the fraction of sodium channels whose activation is negatively shifted by 200 nM Css IV, but not as much as the mutations of the gating charges R850Q and R853Q (Fig. 7d (49)). However, among these mutations of hydrophobic residues in IIS4, only L854C causes a negative shift in voltage dependence, and only L854C gave a CssIV-induced negative shift in the activation curve without a prepulse (Fig. 7b, c) . Interestingly, this mutation is adjacent to R853 where substitutions of C or Q also produced this effect (Fig. 7c; (49)). Altogether, these data highlight the importance of the positively charged and hydrophobic amino acid residues of the IIS4 segment in voltage-dependent activation of sodium channels and in β-scorpion toxin action. R853 and L854 are the most important residues for β-scorpion toxin action, as a mutation at these positions both produce sodium channels whose activation is negatively shifted by Css IV without depolarizing prepulses.

Predicted structure of the β-scorpion toxin/sodium channel complex - In order to gain insight into the three-dimensional structure of the β-scorpion toxin/sodium channel complex, we used the three-dimensional structures of related toxins and ion channels to construct a model of the toxin-channel complex. We modeled the structure of CssIV based on the x-ray crystallographic structure of Centruroides sculpturatus variant II, a structurally related β-scorpion toxin (57). Because the structural scaffold of the scorpion toxins is highly conserved and is made rigid by a set of intramolecular disulfide bonds, it is highly likely that this structural model is accurate and is not altered by binding interactions. We modeled the IIS4 voltage sensor of the sodium channel using the homology/de novo mode of the Rosetta program (see Experimental Procedures) and the x-ray crystallographic structure of the related voltage sensor of the bacterial voltage-gated potassium channel, K_VAP, which was derived from expression and crystallization of the S1 to S4 segments of that channel (29). The resulting structural model predicts that the Css IV toxin fits tightly into the crevice between the S1-S2 and S3-S4 helical hairpins of the sodium channel IIS1-S4 structure and makes close interactions with the amino acid residues shown here to be critical for toxin binding and action (Fig. 8a).

The best Rosetta model shows that that residues E837 and L840 in the IIS3-S4 loop make productive binding interactions with amino acid residues in the Css IV toxin (Fig. 8b). E837 forms a salt bridge with R27 and has a secondary charge-π interaction with Y24. L840 also interacts with Y24 and secondarily with E28 (Fig. 8b). Rotating the model 60^o reveals E779 in the IIS1-S2 loop, which makes a productive charge-π interaction with F44 of Css IV and also interacts with L19 (Fig. 8c). Although these interactions between two pairs of E and L residues initially seemed surprising, interactions between E and L are very common in protein-protein interfaces of known structure (67) and therefore must be quite favorable for binding interactions. All six of these predicted interactions are consistent with mutagenesis results, as we have found important effects of mutations of E779, E 837, and L840 on Css IV binding and action on the sodium channel in this work and Cohen et al. have reported important effects of mutations of L19, Y24, R27, E28, and F44 for binding and toxicity of Css IV (68). The close fit between the structural model and the results of mutagenesis studies strongly supports the accuracy of the structure prediction.

Our previous results also revealed a crucial role for G845 in the sodium channel. Mutation of this residue to N decreased toxin-binding affinity by 13-fold and completely prevented voltage sensor trapping, even when high concentrations of toxin were tested (48). Our

model reveals the molecular basis for this strong effect (Fig. 8d). Even though G845 does not make a productive interaction with Css IV itself, substitution of the much larger N residue creates a steric conflict with the side chains of N7 and F14 of Css IV, which would reduce toxin binding affinity and potentially prevent voltage sensor trapping. Thus, this correlation also supports the accuracy of our structural model.

DISCUSSION

Our results provide crucial new insights into the state-dependence of β-scorpion toxin binding and action, the structure of toxin-receptor complex with the IIS4 voltage sensor of sodium channels, and the molecular mechanism of voltage sensing by the voltage sensors of the voltage-gated ion channel superfamily.

Binding of Css IV to the resting state of sodium channels and voltage-sensor trapping - The β-scorpion toxin Css IV binds to its receptor site in sodium channels in a bimolecular reaction with a K_d in the nanomolar range (48), without markedly altering the activation of the channel. Subsequently, in a rapid, concentration-independent, zero-order state transition of the toxin-channel complex (Figs. 1 and 2), strong depolarization drives the channel into the activated state and the pre-bound toxin locks the IIS4 voltage sensor in its activated conformation. Further depolarizations yield enhanced channel activation because one of the voltage sensors is already locked in the activated conformation. This two-step voltage sensor trapping mechanism allows the toxin to bind at the resting membrane potential yet strongly enhance repetitive action potential firing to produce spastic paralysis of prey. Because of their two-step mechanism of action, the β-scorpion toxins provide unique probes of the structure and function of the IIS4 voltage sensor in both its resting and activated conformations.

Amino acid residues in the IIS1-S2 and IIS3-S4 loops form the β-scorpion toxin receptor site - Mutations of two acidic amino acid residues and one hydrophobic residue in loops IIS1-S2 and IIS3-S4 reduce the affinity of Css IV for its receptor site on sodium channels. The identification of E779 in IIS1-S2 and E837 and L840 in IIS3-S4 as important molecular determinants for ß-scorpion toxin binding on sodium channels suggests that electrostatic and hydrophobic interactions between these amino acid residues and the basic and hydrophobic residues of the toxin are important for toxin binding. To test this idea, we constructed a molecular model of the toxin-receptor interaction, using known x-ray crystal structures of the separate voltage-sensing domain of K_VAP including the S1 to S4 segments (30) and the Centruroides sculpturatus variant II toxin (68). In this structure, the interactive face of the β-scorpion toxin is inserted between the S1-S2 loop and the S3-S4 loop, and the amino acid residues known to be important for binding on the toxin and on the channel interact directly in the binding interface. This mode of interaction allows the toxin to control the relative movement of these two extracellular loops and thereby potentially influence the gating movements of the S4 voltage sensor. Based on this structural model, we propose that movement of the IIS4 segment under the influence of the electric field allows new interactions between the channel and the Css IV toxin. This strengthened toxin-receptor interaction would then stabilize the voltage sensor in its activated conformation and enhance subsequent activation of the sodium channel by negatively shifting its voltage dependence.

A novel binding motif for β-scorpion toxins - Several gating-modifier toxins that inhibit activation or inactivation gating also bind to their target ion channel through interactions with acidic and hydrophobic amino acid residues in S3-S4 loops, which include a key glutamate residue that is conserved at the extracellular end of the S3 segment (35,39,40,48,69-71).

Scheme 1

```
NaIV  YFTIGWNIFDIVVVILSIVGMFLAELIEKYFV---SPTLFRVIRLARIGRILRLIKGAK
Drk1  FFKGPLNAIDLLAILPYYVTIFLTESNKSVLQFQNVRRVVQIFRIMRILRILKLARHST
CaIV  YFRDAWNIFDFVTVLGSITDILVTEFGNNFIN----LSFLRLFRAARLIKLLRQGYTIR
                    S3                                  S4

NaII  YFQEGWNIFDGFIVTLSLVELGLANVEG----------LSVLRSFRLLRVFKLAKSWP
```

Scheme 1 illustrates the alignment of the S3 segments and the S3-S4 loops in domain IV of $Na_V1.2$ channels containing the α-scorpion toxin and sea anemone toxin receptor sites, in domain IV of $Ca_V2.1$ channels containing the ω-agatoxin receptor site, and in the Drk1 K^+ channel containing the hanatoxin and grammotoxin receptor sites. This alignment reveals a common toxin binding motif at the extracellular end of the S3 segment composed of 2 hydrophobic residues and 1 acidic residue in the sequence ΦΦXXE (Scheme 1, shaded residues). In contrast, the amino acid residues involved in the formation of the ß-scorpion toxin receptor site on IIS3-S4 linker of $Na_v1.2$ channels are quite different in sequence context (Scheme 1). β-scorpion toxins are the first group of gating modifier toxins to interact with a different binding motif in the S3-S4 linker, and they are unique in enhancing activation of their target channel. Further insights concerning the mechanism of activation of voltage-gated ion channels may emerge from studies of complexes of the β-scorpion toxins with sodium channel IIS4 voltage sensor in different functional states.

Functional role of positively charged and hydrophobic amino acid residues in the S4 segment of domain II in activation and toxin modification - Previous mutagenesis studies of the S4 segments of $Na_V1.2$ channels have focused on the positively charged residues, which serve as gating charges. Among the hydrophobic residues in transmembrane segment IIS4 of sodium channels, only L860 has been shown previously to be involved in activation (51). In this work, we analyzed the effects of mutations of all of the hydrophobic amino acid residues of the S4 segment in domain II and compared their effects with previous work on the positively charged residues. Surprisingly, all of our mutations of hydrophobic residues affect activation gating significantly (Fig. 7b). Mutations of seven of the hydrophobic residues in the IIS4 segment shift the voltage dependence of activation in the positive direction, opposing the transition to the activated state. In contrast, mutation L854C shifts activation in the negative direction and therefore favors activation. In addition, the slope of the activation curve is reduced for all these point mutants, suggesting that the total transmembrane movement of gating charge is reduced by these mutations, even though these amino acid residues cannot themselves carry gating charge. Illustration of the IIS4 segment as a helical net (Fig. 7) reveals that the seven hydrophobic amino acid residues whose mutation opposes activation are arrayed around most of the circumference of the alpha helix. These results suggest that the native hydrophobic residues in these positions favor activation, perhaps by forming stronger hydrophobic interactions with the surrounding transmembrane alpha helices in the activated state. Similarly, mutations of each positively charged residue in the transmembrane segment shift the voltage dependence of activation to more positive potentials, indicating that the native amino acid residues make interactions that favor the activated state. In contrast, mutation of L854 favors activation, suggesting that this native residue makes hydrophobic interactions that are more stable in the closed state and therefore reduce activation (Fig. 7b). Evidently, the precise topology and chemical properties of both the positively charged and hydrophobic amino acid residues are critical to allow a correct fit of the S4 segment into its surrounding transmembrane environment, and therefore, changes of any of the hydrophobic amino acid residues have an important effect on gating as we have observed.

Role of IIS4 residues in voltage-sensor trapping and ß-scorpion toxin action - Mutations of the positively charged and hydrophobic amino acid residues in the IIS4 segment do not alter the binding affinity of Css IV for its receptor site ((49) and this work), suggesting that there are no direct interactions between the toxin and the IIS4 segment in the resting state. However, although mutations in the IIS4 segment do not alter Css IV binding, they do have important effects on its functional consequences. Our previous work showed that neutralization of R850 and R853 strongly enhances the toxin-induced negative shift in the voltage dependence of channel activation ((49) and Fig. 7). The present data indicate that mutation of the hydrophobic residues V848, F852, L854 and V857 in the IIS4 voltage sensor also favors ß-scorpion toxin enhancement of sodium channel activation. All of these mutations increase the fraction of sodium channels that have negatively shifted activation gating, and mutation of L854 allows the Css IV toxin to induce a negative shift in the voltage dependence of activation without a prepulse, as previously observed for mutation of R853 ((49) and Fig. 7). These results suggest that both electrostatic interactions of R850 and R853 with negatively charged amino acid residues and hydrophobic interactions of V848, F852, L854, and V857 with neighboring transmembrane segments are important for stabilizing the IIS4 segment in its inward, resting conformation. Mutations of these amino acid residues evidently reduce the kinetic barrier for S4 movement, increasing the probability for the IIS3-S4 loop and IIS4 segment to be exposed at the extracellular side of the membrane, which favors ß-scorpion toxin trapping of the IIS4 segment in its activated position.

Implications for the molecular mechanism of voltage sensing - The position of the S4 voltage sensor in the resting state of the sodium channel is a key point of controversy in studies of the molecular mechanism of voltage sensing (23,72,73). The X-ray structure of a bacterial voltage-dependent potassium channel (KvAP) in complex with detergent and a site-directed antibody against the S3-S4 loop predicts that the S1-S2 and S3-S4 loops would be positioned at the intracellular surface of the membrane in the resting state (29,30). Based on this structure, a 'paddle' model of voltage sensing has been proposed, in which the S1-S4 voltage sensor structure lies separate from the core of the channel protein along the intracellular surface of the membrane in the resting state and pivots as a rigid unit across the membrane and binds to the core of the channel during activation. Only after channel activation would the S1-S2 and S3-S4 loops become exposed to the external side in response to depolarization and become available for toxin binding in this gating model. Our results are not consistent with this gating model. We show that Css IV toxin binds to the sodium channel in the resting state. Its binding involves amino acid residues in the IIS1-S2 and IIS3-S4 loops. Our structural model of the toxin-receptor complex shows that the crevice formed by the S1-S2 and the S3-S4 helical hairpins accommodates all of the interactive surface of the toxin that has been defined by mutagenesis studies, arguing against any other significant interaction sites in the resting state. The Css IV toxin is a hydrophilic, 70-residue polypeptide that has charged amino acid residues on its interactive surface, making its penetration through the lipid bilayer highly unlikely. Altogether, these experimental results indicate that the Css IV toxin binds to the S1-S2 and the S3-S4 loops on the extracellular surface of the membrane in the resting state of the sodium channel. These results argue against voltage-sensing models in which the IIS4 voltage sensor of sodium channels is in an intracellular or intramembrane position in the resting state. As the structures of the S4 segments of the voltage-gated ion channels are conserved across over 80 members of this protein superfamily (1), it is highly likely that this conclusion holds for all of the voltage sensors in these channels.

Consistent with our structural model for the β-scorpion toxin/voltage sensor complex, a recent x-ray crystallographic structure of the $K_V1.2$ channel in complex with its $K_V\beta$ subunit reveals the S4 voltage sensor in a transmembrane position with the S3-S4 linker present on the extracellular surface of the channel protein in the activated state (74). Together with our results showing the S3-S4 linker in an extracellular

position in the resting state of the $Na_V1.2$ channel, these results imply that the S4 voltage sensor retains a transmembrane position in both resting and activated states and transfers gating charge across the membrane by a helical movement through the protein rather than by a paddle movement through the lipid. Further understanding the molecular details of the voltage sensor trapping mechanism of Css IV toxin should give new insights into the mechanisms of voltage sensing and activation gating of the ion channel protein superfamily.

REFERENCES

1. Yu, F. H., and Catterall, W. A. (2004) *Sci STKE* **2004**(253), re15
2. Hodgkin, A. L., and Huxley, A. F. (1952) *J. Physiol.* **117**, 500-544
3. Catterall, W. A. (1980) *Annu. Rev. Pharmacol. Toxicol.* **20**, 15-43
4. Cestèle, S., and Catterall, W. A. (2000) *Biochimie* **82**(9), 883-892
5. Catterall, W. A. (2000) *Neuron* **26**(1), 13-25
6. Morgan, K., Stevens, E. B., Shah, B., Cox, P. J., Dixon, A. K., Lee, K., Pinnock, R. D., Hughes, J., Richardson, P. J., Mizuguchi, K., and Jackson, A. P. (2000) *Proc. Natl. Acad. Sci. U. S. A.* **97**(5), 2308-2313
7. Yu, F. H., Westenbroek, R. E., Silos-Santiago, I., McCormick, K. A., Lawson, D., Ge, P., Ferriera, H., Lilly, J., DiStefano, P. S., Catterall, W. A., Scheuer, T., and Curtis, R. (2003) *J. Neurosci.* **23**(20), 7577-7585
8. Armstrong, C. M. (1981) *Physiol. Rev.* **61**, 644-682
9. Catterall, W. A. (1986) *Annu. Rev. Biochem.* **55**, 953-985
10. Stuhmer, W., Conti, F., Suzuki, H., Wang, X., Noda, M., Yahadi, N., Kubo, H., and Numa, S. (1989) *Nature* **339**, 597-603
11. Yang, N., and Horn, R. (1995) *Neuron* **15**, 213-218
12. Yang, N. B., George, A. L., Jr., and Horn, R. (1996) *Neuron* **16**, 113-122
13. Chen, L. Q., Santarelli, V., Horn, R., and Kallen, R. G. (1996) *J. Gen. Physiol.* **108**, 549-556
14. Chanda, B., and Bezanilla, F. (2002) *J. Gen. Physiol.* **120**(5), 629-645
15. Guy, H. R., and Seetharamulu, P. (1986) *Proc. Natl. Acad. Sci. U. S. A.* **508**, 508-512
16. Liman, E. R., Hess, P., Weaver, F., and Koren, G. (1991) *Nature* **353**, 752-756
17. Papazian, D. M., Shao, X. M., Seoh, S. A., Mock, A. F., Huang, Y., and Wainstock, D. H. (1995) *Neuron* **14**, 1293-1301
18. Seoh, S. A., Sigg, D., Papazian, D. M., and Bezanilla, F. (1996) *Neuron* **16**(6), 1159-1167
19. Cha, A., Ruben, P. C., George, A. L., Fujimoto, E., and Bezanilla, F. (1999) *Neuron* **22**, 73-87
20. Larsson, H. P., Baker, O. S., Dhillon, D. S., and Isacoff, E. Y. (1996) *Neuron* **16**, 387-397
21. Yang, N. B., George, A. L., and Horn, R. (1997) *Biophys. J.* **73**, 2260-2268
22. Starace, D. M., and Bezanilla, F. (2004) *Nature* **427**(6974), 548-553
23. Ahern, C. A., and Horn, R. (2004) *J. Gen. Physiol.* **123**(3), 205-216
24. Starace, D. M., and Bezanilla, F. (2001) *J. Gen. Physiol.* **117**(5), 469-490
25. Tombola, F., Pathak, M. M., and Isacoff, E. Y. (2005) *Neuron* **45**(3), 379-388
26. Sokolov, S. (2005) *Neuron* **47**, 183-189
27. Sato, C., Ueno, Y., Asai, K., Takahashi, K., Sato, M., Engel, A., and Fujiyoshi, Y. (2001) *Nature* **409**(6823), 1047-1051
28. Jiang, Q. X., Wang, D. N., and MacKinnon, R. (2004) *Nature* **430**(7001), 806-810
29. Jiang, Y., Lee, A., Chen, J., Ruta, V., Cadene, M., Chait, B. T., and MacKinnon, R. (2003) *Nature* **423**(6935), 33-41
30. Jiang, Y., Ruta, V., Chen, J., Lee, A., and MacKinnon, R. (2003) *Nature* **423**(6935), 42-48
31. Catterall, W. A. (1977) *J. Biol. Chem.* **252**, 8660-8668
32. Catterall, W. A. (1979) *J. Gen. Physiol.* **74**, 375-391

33. Catterall, W. A., and Beress, L. (1978) *J. Biol. Chem.* **253**, 7393-7396
34. Nicholson, G. M., Willow, M., Howden, M. E. H., and Narahashi, T. (1994) *Pflügers Arch.* **428**, 400-409
35. Rogers, J. C., Qu, Y., Tanada, T. N., Scheuer, T., and Catterall, W. A. (1996) *J. Biol. Chem.* **271**, 15950-15962
36. Tejedor, F. J., and Catterall, W. A. (1988) *Proc. Natl. Acad. Sci. U. S. A.* **85**, 8742-8746
37. Thomsen, W. J., and Catterall, W. A. (1989) *Proc. Natl. Acad. Sci. U. S. A.* **86**, 10161-10165
38. Sheets, M. F., Kyle, J. W., Kallen, R. G., and Hanck, D. A. (1999) *Biophys. J.* **77**, 747-757
39. Bourinet, E., Soong, T. W., Sutton, K., Slaymaker, S., Matthews, E., Monteil, A., Samoni, G. W., Nargeot, J., and Snutch, T. P. (1999) *Nat. Neurosci.* **2**, 407-415
40. Swartz, K. J., and MacKinnon, R. (1997) *Neuron* **18**, 675-682
41. Cahalan, M. D. (1975) *J. Physiol.* **244**, 511-534
42. Jover, E., Couraud, F., and Rochat, F. (1980) *Biochem. Biophys. Res. Commun.* **95**, 1697-1714
43. Jaimovich, E., Ildefonse, M., Barhanin, J., Rougier, O., and Lazdunski, M. (1982) *Proc. Natl. Acad. Sci. U. S. A.* **79**(12), 3896-3900
44. Meves, H., Rubly, N., and Watt, D. D. (1982) *Pflügers Arch. Physiol.* **393**, 56-62
45. Wang, G. K., and Strichartz, G. R. (1983) *Mol. Pharmacol.* **23**(2), 519-533
46. Vijverberg, H. P., Pauron, D., and Lazdunski, M. (1984) *Pflügers Arch.* **401**(3), 297-303
47. Jonas, P., Vogel, W., Arantes, E. C., and Giglio, J. R. (1986) *Pflugers Arch.* **407**(1), 92-99
48. Cestèle, S., Qu, Y., Rogers, J. C., Rochat, H., Scheuer, T., and Catterall, W. A. (1998) *Neuron* **21**, 919-931
49. Cestèle, S., Scheuer, T., Mantegazza, M., Rochat, H., and Catterall, W. A. (2001) *J. Gen. Physiol.* **118**, 291-302
50. Martin-Eauclaire, M. F., Garcia y Perez, L. G., el Ayeb, M., Kopeyan, C., Bechis, G., Jover, E., and Rochat, H. (1987) *J. Biol. Chem.* **262**(10), 4452-4459
51. Auld, V. J., Goldin, A. L., Krafte, D. S., Catterall, W. A., Lester, H. A., Davidson, N., and Dunn, R. J. (1990) *Proc. Natl. Acad. Sci. U.S.A.* **87**, 323-327
52. Goldin, A. L., Barchi, R. L., Caldwell, J. H., Hofmann, F., Howe, J. R., Hunter, J. C., Kallen, R. G., Mandel, G., Meisler, M. H., Berwald Netter, Y., Noda, M., Tamkun, M. M., Waxman, S. G., Wood, J. N., and Catterall, W. A. (2000) *Neuron* **28**, 365-368
53. Kunkel, T. A. (1985) *Proc. Natl. Acad. Sci. U. S. A.* **82**, 488-492
54. Margolskee, R. F., McHendry-Rinde, B., and Horn, R. (1993) *Biotechniques* **15**, 906-911
55. Ruta, V., Jiang, Y., Lee, A., Chen, J., and MacKinnon, R. (2003) *Nature* **422**(6928), 180-185
56. Jeanmougin, F., Thompson, J. D., Gouy, M., Higgins, D. G., and Gibson, T. J. (1998) *Trends Biochem. Sci.* **23**(10), 403-405
57. Cook, W. J., Zell, A., Watt, D. D., and Ealick, S. E. (2002) *Protein Sci.* **11**(3), 479-486
58. Clamp, M. E., Cuff, J. A., and Barton, G. J. (1999) Jalview- a java multiple sequence alignment viewer and editor http://www.ebi.ac.uk/~michele/jalview/. In.
59. Simons, K. T., Ruczinski, I., Kooperberg, C., Fox, B. A., Bystroff, C., and Baker, D. (1999) *Proteins* **34**(1), 82-95
60. Simons, K. T., Kooperberg, C., Huang, E., and Baker, D. (1997) *J. Mol. Biol.* **268**(1), 209-225
61. Rohl, C. A., Strauss, C. E., Chivian, D., and Baker, D. (2004) *Proteins* **55**(3), 656-677
62. Rohl, C. A., Strauss, C. E., Misura, K. M., and Baker, D. (2004) *Methods Enzymol.* **383**, 66-93
63. Gray, J. J., Moughon, S., Wang, C., Schueler-Furman, O., Kuhlman, B., Rohl, C. A., and Baker, D. (2003) *J. Mol. Biol.* **331**(1), 281-299
64. Darbon, H., and Angelides, K. J. (1984) *J Biol Chem* **259**(10), 6074-6084
65. Hassani, O., Mansuelle, P., Cestele, S., Bourdeaux, M., Rochat, H., and Sampieri, F. (1999) *Eur J Biochem* **260**(1), 76-86

66. Cohen, L., Karbat, I., Gilles, N., Froy, O., Corzo, G., Angelovici, R., Gordon, D., and Gurevitz, M. (2004) *J Biol Chem* **279**(9), 8206-8211
67. Glaser, F., Steinberg, D. M., Vakser, I. A., and Ben-Tal, N. (2001) *Proteins* **43**(2), 89-102
68. Cohen, L., Karbat, I., Gilles, N., Ilan, N., Benveniste, M., Gordon, D., and Gurevitz, M. (2005) *J. Biol. Chem.* **280**(6), 5045-5053
69. Winterfield, J. R., and Swartz, K. J. (2000) *J. Gen. Physiol.* **116**(5), 637-644
70. Li-Smerin, Y., and Swartz, K. J. (2000) *J. Gen. Physiol.* **115**(6), 673-684
71. Li-Smerin, Y., and Swartz, K. J. (1998) *Proc. Natl. Acad. Sci. U. S. A.* **95**(15), 8585-8589
72. Bezanilla, F. (2005) *Trends Biochem. Sci.* **30**(4), 166-168
73. Laine, M., Lin, M. C., Bannister, J. P., Silverman, W. R., Mock, A. F., Roux, B., and Papazian, D. M. (2003) *Neuron* **39**(3), 467-481
74. Long, S. B., Campbell, E. B., and Mackinnon, R. (2005) *Science* **309**(5736), 903-908

FOOTNOTES

We are grateful to Prof. Hervé Rochat (CNRS UMR 6560, Marseille, France) for his constant support. We thank Dr. Pierre E. Bougis and Brigitte Céard (CNRS UMR 6560, Marseille, France) for their help and Dr. Marie-France Martin-Eauclaire (CNRS UMR 6560, Marseille, France) for purifying the ß-scorpion toxin Css IV. The work at the University of Washington was supported by NIH Research Grants R01 NS15751 to W. A. C. and MH67625 to V. Y.-Y.

FIGURE LEGENDS

Fig. 1. Rapid modification of voltage-dependent activation by pre-bound Css IV. In the presence of 200 nM Css IV, currents activated much faster elicited after a conditioning prepulse. Currents were elicited at the potentials indicated from a holding potential of –100 mV either with a +50 mV, 1 ms prepulse applied 60 ms before the test pulse (gray line, larger current), or without a prepulse (black line, smaller current). Dotted lines are the scaled version of current elicited without prepulse.

Fig. 2. Dependence of the rate of shift of the voltage dependence of activation on Css IV concentration. Currents were elicited at –65 mV, 60 ms after conditioning pulses to +20 mV of variable duration (0.1 (smallest current) to 1.4 s (largest current). (a) In the presence of 40 nM Css IV; (b) In the presence of 400 nM Css IV; (c) Current amplitude plotted against the duration of conditioning pulse in the presence of 40 nM Css IV (filled circles) or 400 nM Css IV (filled squares). The open circles are a scaled version of the 40 nM data. The solid lines are single exponential fits to the data with time constants of 0.412 ms (40 nM Css IV) and 0.402 ms (400 nM Css IV). Note that the amount of current elicited at –65 mV in 400 nM Css IV is greater than in 40 nM Css IV. (d) Time constants for development of currents at -65 mV at conditioning pulses of 20 mV, 50 mV and 80 mV in the presence of 40 nM (white) or 400 nM (gray) Css IV.

Fig. 3. Binding affinity of Css IV for wild-type and mutant $Na_v1.2$ channels. Wild-type and mutant Nav1.2 channels were transiently expressed in tsA-201 cells and binding affinity for CssIV toxin was measured as described under Experimental Procedures. (a) Competitive binding curves for inhibition of ^{125}I-Css IV binding to transiently expressed channels by unlabeled Css IV for transiently expressed Nav1.2 (filled circles) and E779Q channels (open circles, $K_{d\ (E779Q)}$= 0.46 ± 0.04 nM). (b) Competitive binding curves for inhibition of ^{125}I-Css IV binding to transiently expressed sodium channels by unlabeled

Css IV for transiently expressed $Na_V1.2$ (filled circles), E837Q (open squares; $K_{d\ (E837Q)}$= 0.56 ± 0.12 nM) and L840C channels ($K_{d\ (L840C)}$= 0.0.68 ± 0.04 nM). (c) Bar graph illustrating K_d values for all mutants.

Fig. 4. Functional properties and activity of Css IV on mutant Nav1.2 channels with altered toxin affinity. (a) Voltage dependence of activation for wild-type $Na_v1.2$, E779Q, E837Q and L840C channels and for wild-type with 200 nM Css IV. Conductance-voltage relationships were determined as described under Experimental Procedures. (b-d) Conductance-voltage relationships measured in control (closed symbols) and in the presence of 200 nM Css IV with a +50 mV, 1 ms prepulse preceding the test pulse by 60 ms for E779Q (b), E837Q (c) and L840C (d) channels. Analogous data in the presence of 1 μM Css IV are shown for E779Q (b) and L840C (d) as gray symbols.

Fig. 5. Effects of mutations of hydrophobic residues in the IIS4 segment on sodium channel activation. Voltage dependence of activation for wild-type $Na_v1.2$, E779Q, E837Q and L840C channels. Conductance-voltage relationships were determined as described under Experimental Procedures.

Fig. 6. Activity of Css IV on Nav1.2 channels with mutations of hydrophobic amino acid residues in the IIS4 segment. Conductance-voltage relationships of wild type $Na_v1.2$ and mutant channels in the presence of 200 nM Css IV with a 1-ms prepulse to +50 mV that preceded the test pulse by 60 ms. (a) Nav1.2, V484A, and L849C. (b) Nav1.2, F852A, and L855C. (c) Nav1.2, L854C/PRE with a prepulse, and L854C/NP without a prepulse. (d) Nav1.2, V857C, F858C, and L860C.

Fig. 7. Functional effects of mutations of amino acid residues in the IIS4 segment.

(a) A helical net depiction of the amino acids of transmembrane segement IIS4. The charged arginines and lysines are highlighted. (b) The shift in the activation curve relative to WT of each IIS4 mutant channels. (c) The percentage of channels shifted negatively in the absence of a prepulse in the presence of 200 nM CssIV for each of the mutant channels as indicated by the fit of a two component Boltzmann equation (see Experimental Procedures). (d) The percentage of channels shifted negatively in the presence of a prepulse in the presence of 200 nM CssIV for each of the mutant channels. Values for R850Q, R853Q, R856Q, and R859Q are from (49).

Fig. 8. Structural model of β-scorpion toxin binding to $Na_v1.2$. Docking model of β-scorpion CssIV toxin binding to the voltage-sensing segments of domain II of $Na_v1.2$, generated as described in Experimental Procedures. (a) Molecular surface representation of the same view of the model as in panel A. To demonstrate overall shape complementation, β-scorpion CssIV toxin model separated from the sodium channel model. Side chains of selected residues labeled with corresponding residue numbers. Side chains colored as white for hydrophobic residues, blue for positively charged residues, red for negatively charged residues and green for polar but uncharged residues. (b) Side view of the ribbon representation of the docking model with the sodium channel transmembrane segments S1 and S4 on the front. Side chains of selected residues shown in stick representation. (c) Side view of the ribbon representation of the docking model with the sodium channel transmembrane segments S1 and S4 on the front. Side chains of residues proposed to be important for Na^+ channel-Css IV interaction shown in stick representation. (d) Side view of the ribbon representation of the docking model with the sodium channel transmembrane segments S1, S2 and S3 on the front. Side chains of residues proposed to be important for Na^+ channel - CssIV interaction shown in stick representation.

Voltage Sensor of Sodium Channels Probed by a β-Scorpion Toxin

Supplementary Tables

Table 1. Voltage-dependence of activation for $Na_v1.2$ and mutant channels in control conditions.

Table 2. Voltage-dependence of activation for $Na_v1.2$ and mutant channels in the presence of 200 nM Css IV.

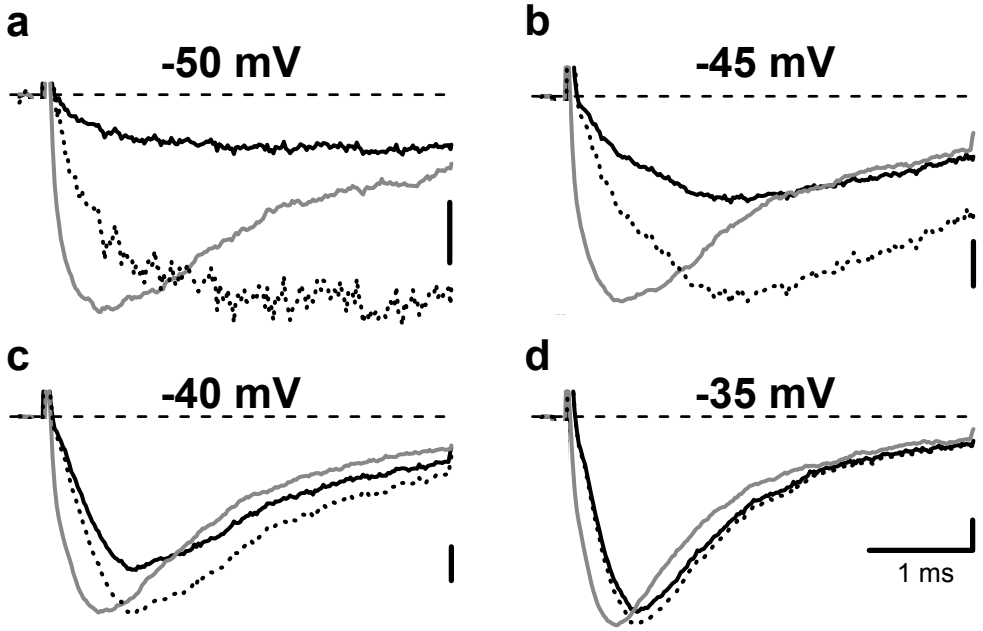

Figure 1
Catterall

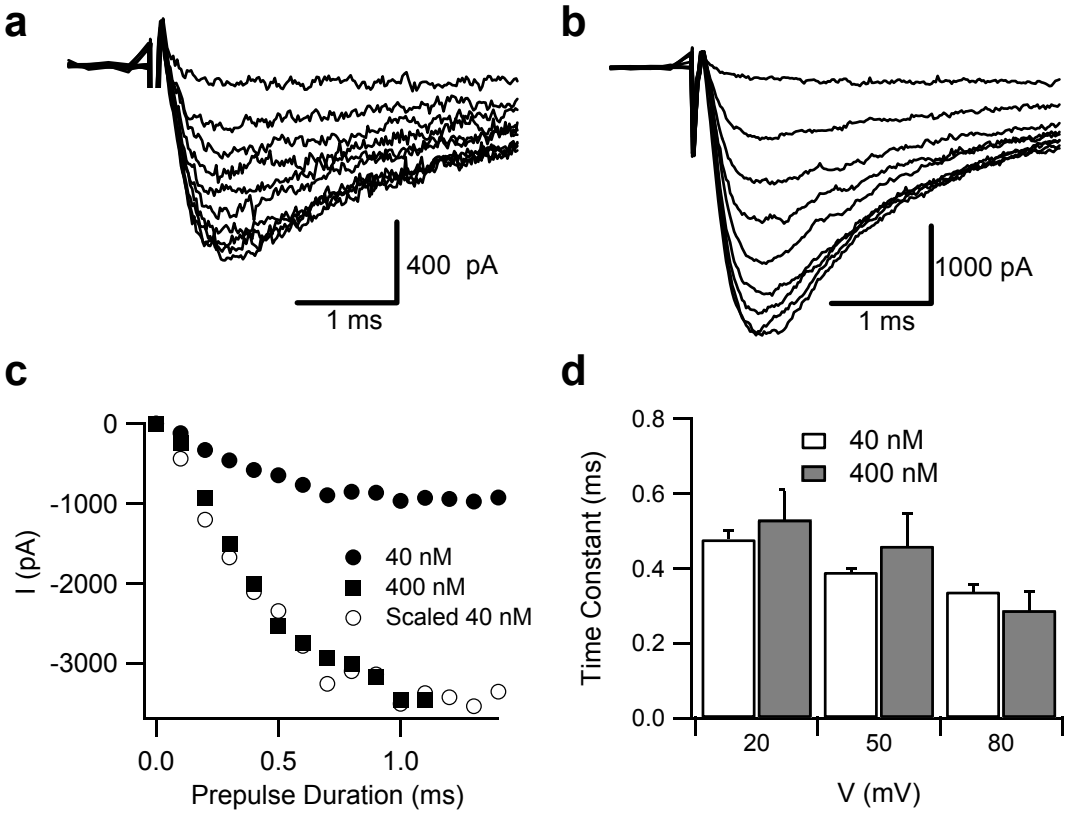

Figure 2

Catterall

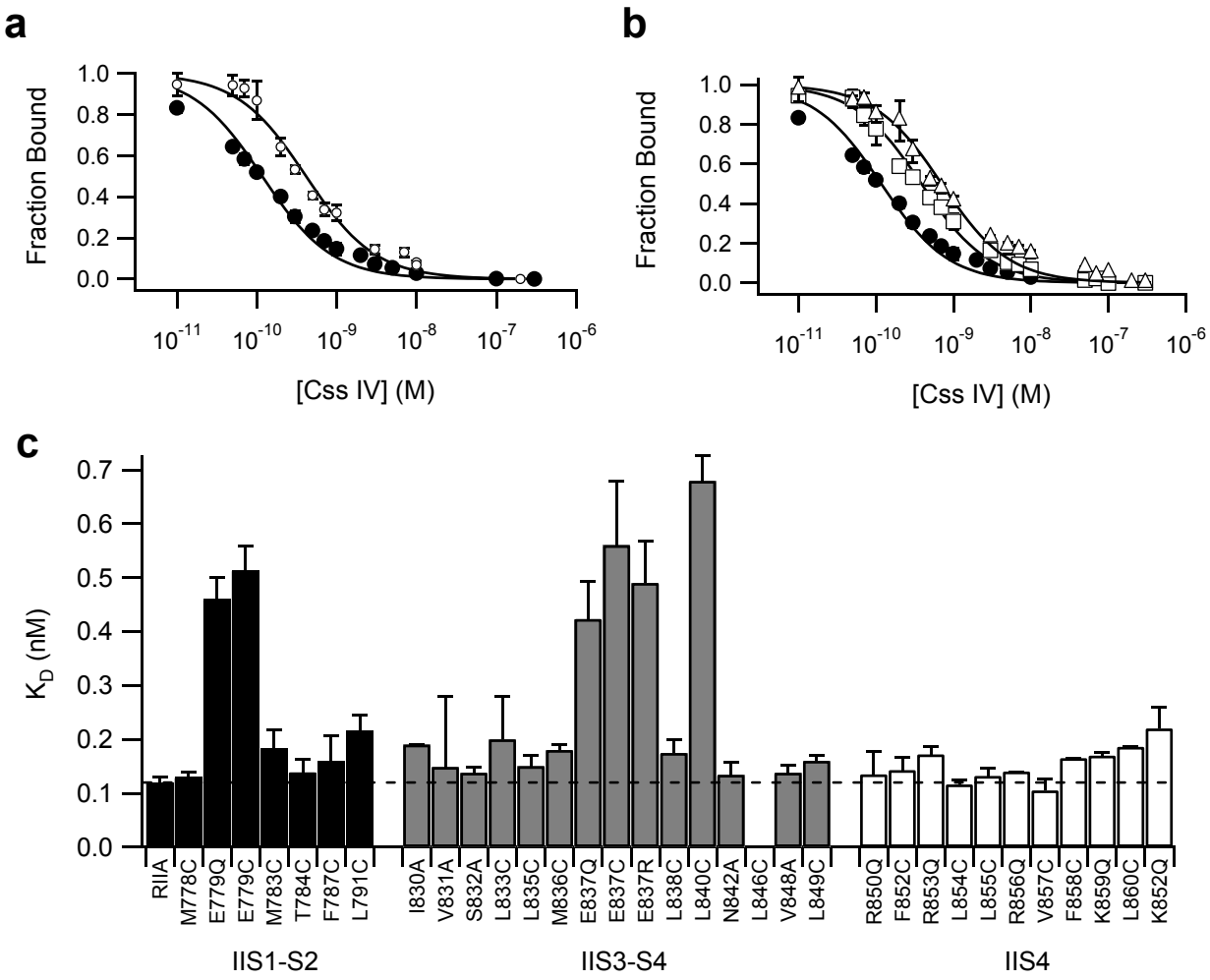

Figure 3
Catterall

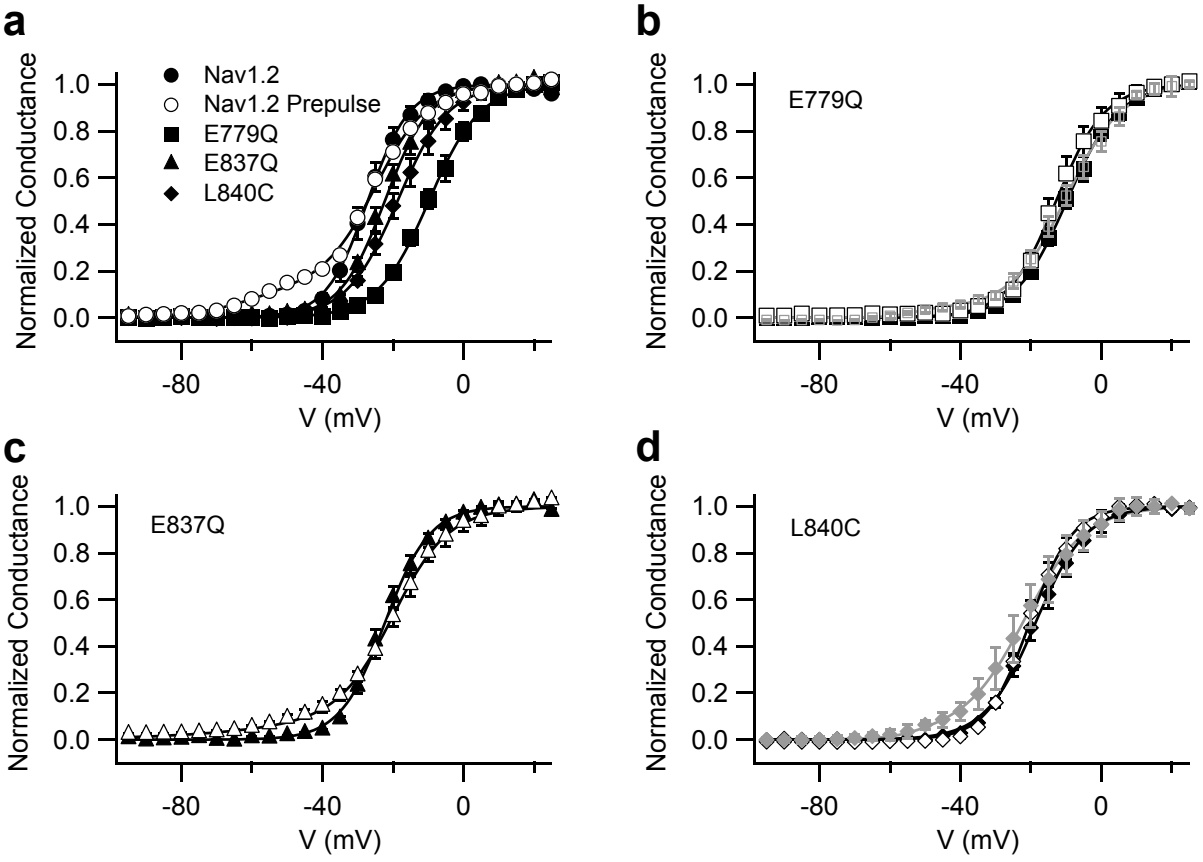

Figure 4

Catterall

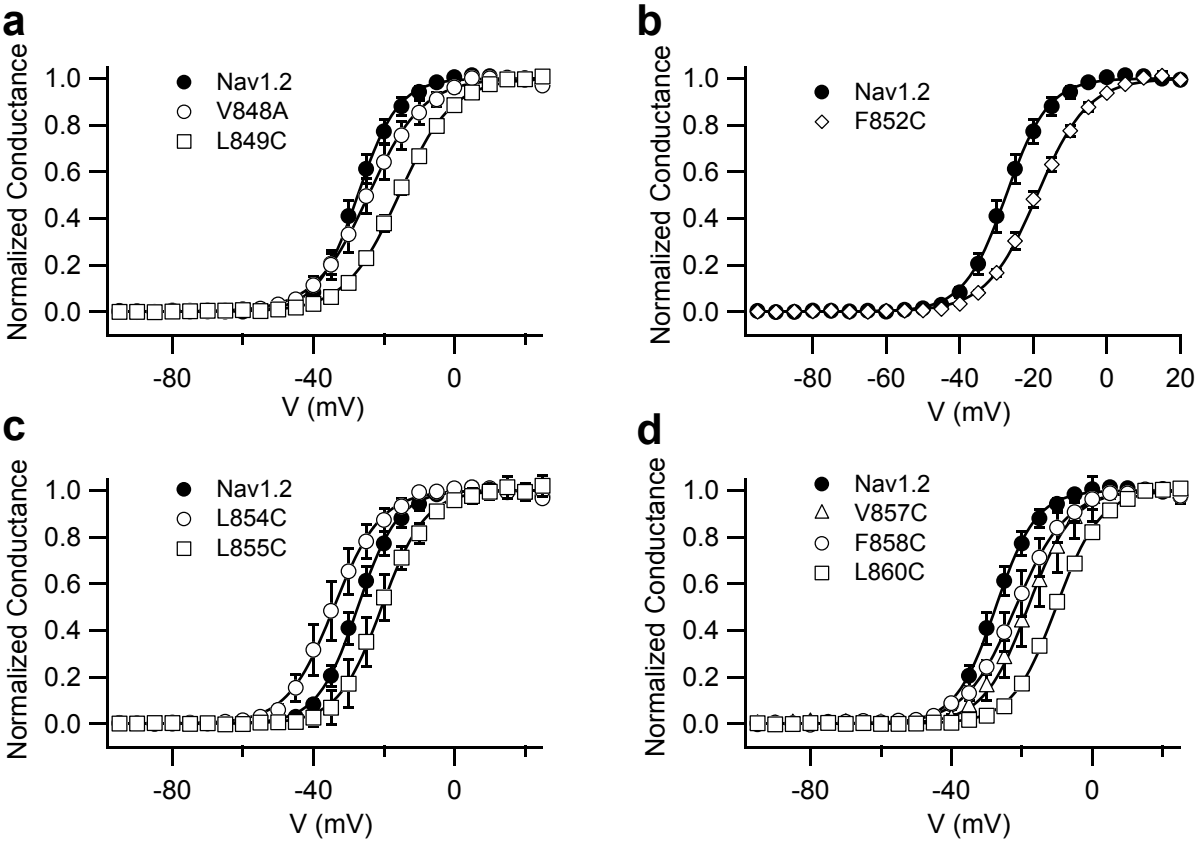

Figure 5

Catterall

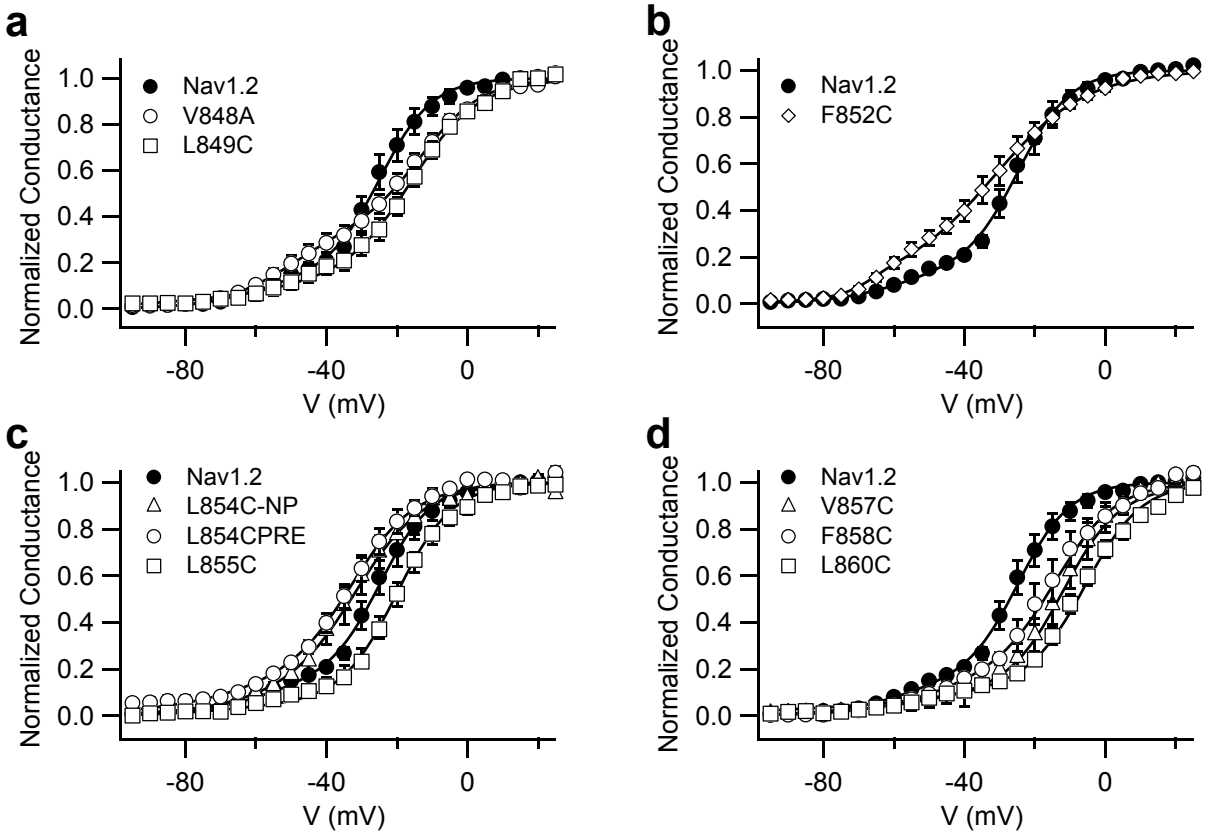

Figure 6

Catterall

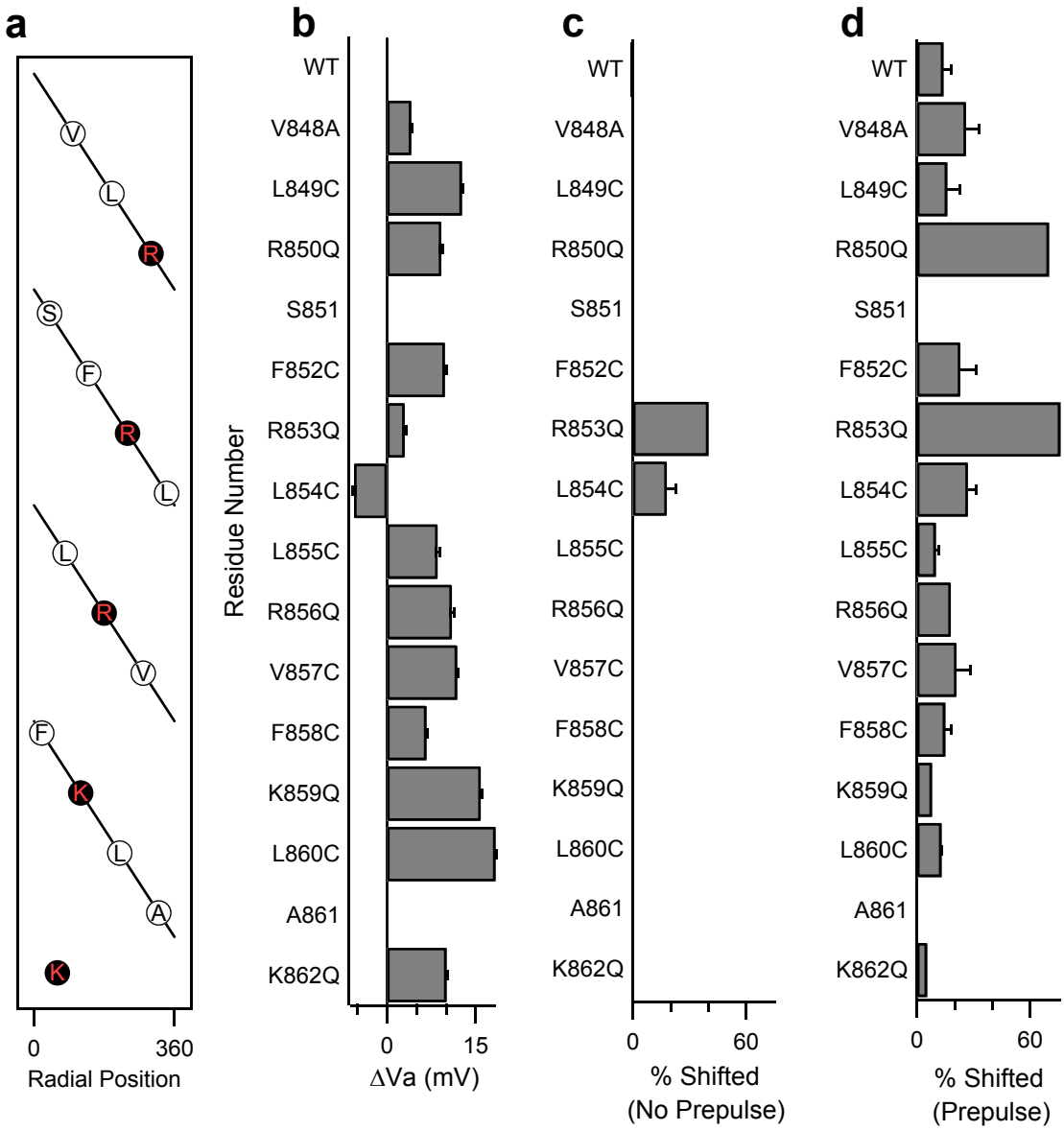

Figure 7

Catterall

Fig. 8A

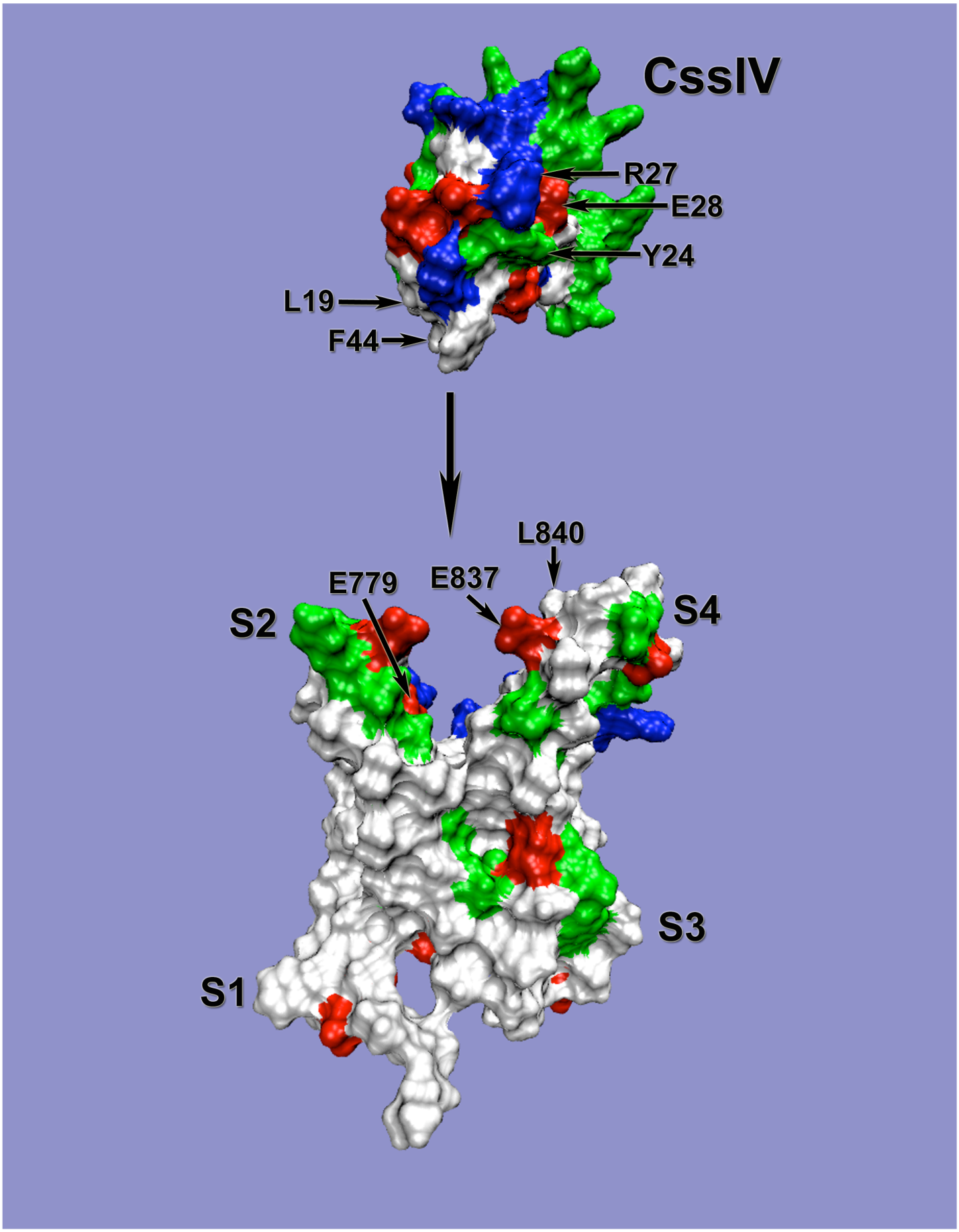

Fig. 8B

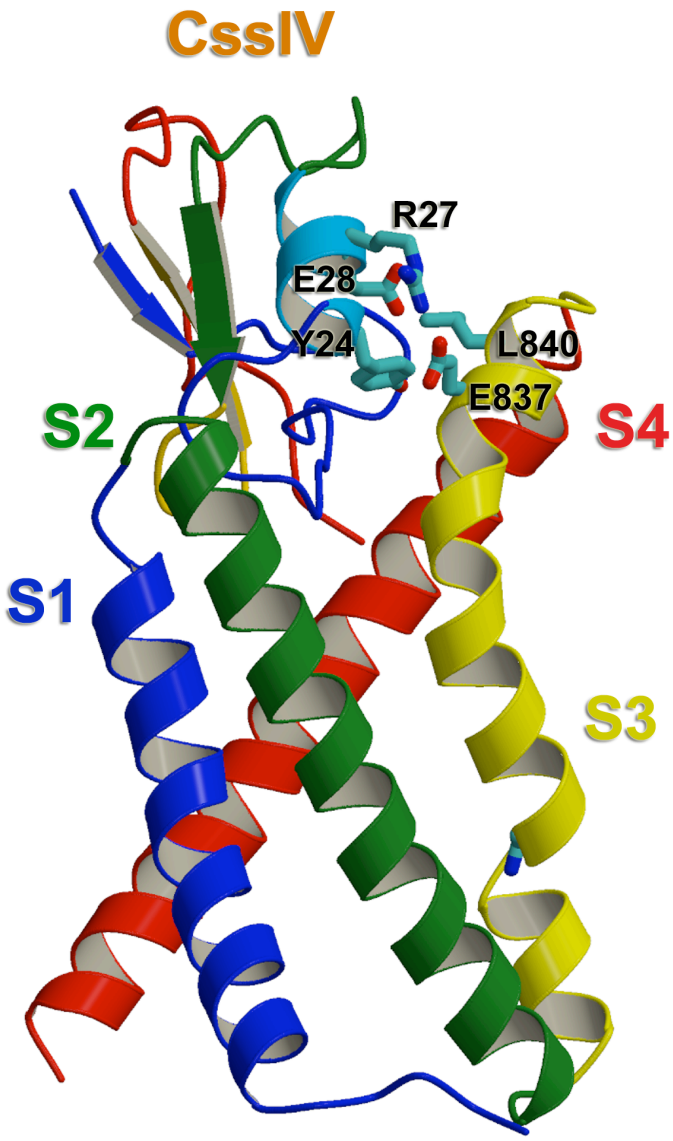

Fig. 8C

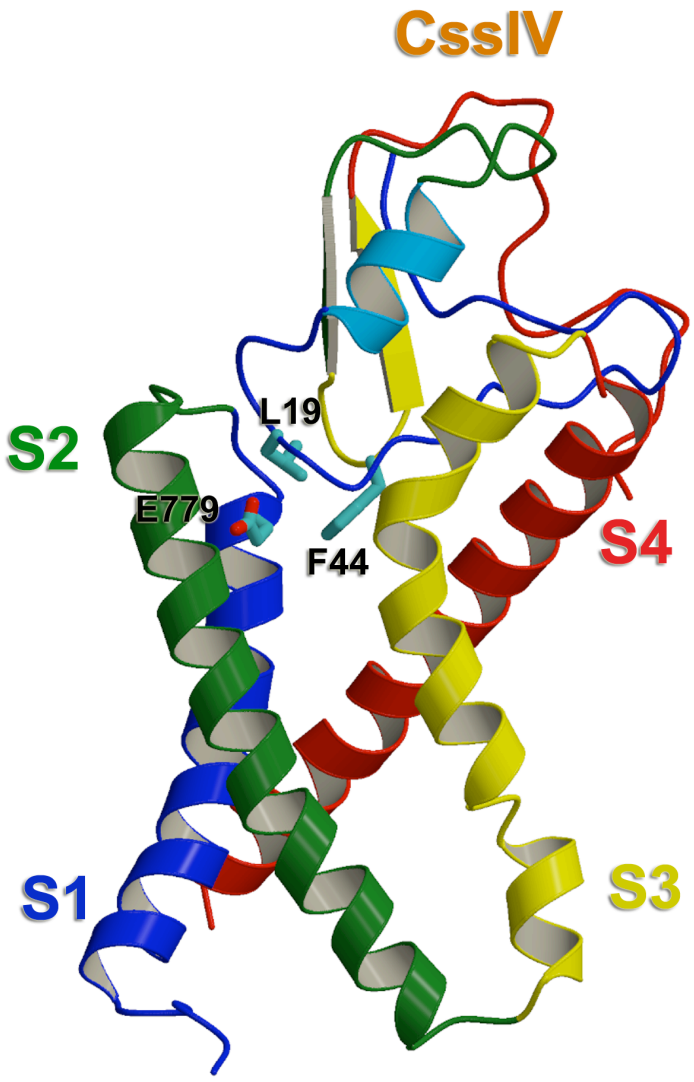

Fig. 8D